Recent Climate Changes in Precipitable Water in the Global Tropics as Revealed in NCEP/NCAR Reanalysis

Igor I. Zveryaev and Pao-Shin Chu*

P.P. Shirshov Institute of Oceanology, RAS, Moscow, Russia

*Department of Meteorology, SOEST, University of Hawaii at Manoa, Honolulu, Hawaii

JGR-Atmospheres(2003, in press)

November 14, 2002

Address for correspondence:

Dr. Pao-Shin Chu, Department of Meteorology, SOEST, University of Hawaii,

2525 Correa Rd., HIG 350, Honolulu, HI 96822-2291, USA

Telephone: 1 (808) 956-8775

Fax: 1 (808) 956-2877

Email: chu@hawaii.edu

Abstract

For the first time, long-term climate changes in the atmospheric moisture over the global tropics are investigated using precipitable water (PW) from the NCEP/NCAR Reanalysis datasets for two different periods: 1979-1998 and 1948-1998. Dominant modes of PW variability estimated for the shorter period (1979-1998) are in an overall agreement with those of satellite-estimated precipitation in terms of both EOF spatial patterns and time-dependent coefficients. Encouraged by this result, the entire time series of PW for the period of 1948-1998 is subsequently examined. Climatology of annual mean PW agrees well with the radiosonde-based and satellite-based climatologies of atmospheric moisture.

EOF analysis applied to the entire time series indicates that the two leading modes explain 37.3 % of the total variance of PW. The first EOF mode reflects that the trend-like change is associated with evolutions in the observing systems of NCEP/NCAR reanalysis product. The second EOF has a spatial pattern which is characterized by the zonal dipole structure. This mode is associated with the major climatic signal in the region - El Niño-Southern Oscillation (ENSO).

Analysis of regional time series of annual mean PW has shown that, coincident with introduction of satellite data, step-like changes in the mid-late 1970s are present over Malaysia, central tropical Pacific, and central Brazil. Abrupt changes of PW over North Africa are noticed in the late 1960s, and the large positive PW anomalies observed during the 1950s and 1960s are suspected to have quality deficiencies.

1. Introduction

Being a key variable of the global climate system, atmospheric water vapor plays a principal role in the hydrological cycle. Radiative effects of the atmospheric water vapor are particularly important. Atmospheric water vapor absorbs strongly a portion of the earth's outgoing infrared energy and radiates this energy back to the earth's surface. Thus, water vapor strengthens the greenhouse effect. Because the atmosphere can hold more water vapor in a warmer climate, an increase in water vapor is believed to lead to increased greenhouse effect by enhancing the warming. During the past two decades, analysis of spatio-temporal variability of the atmospheric moisture has received considerable attention. A number of papers focused on the regional changes in atmospheric water vapor [*Angell et al*., 1984; *Hense et al*., 1988; *Flohn and Kapala*, 1989; *Ross and Elliott*, 1996; *Zhai and Eskridge*, 1997]. Several other studies considered global distribution of the atmospheric moisture and its variability [*Oort*, 1983; *Peixoto and Oort*, 1992; *Gaffen et al*., 1991]. Most of the aforementioned studies are based on analysis of radiosonde data, which provide relatively long time series of observations. However, radiosonde measurements are made primarily over land and are widely spaced.

Another promising data source for atmospheric moisture is satellite-based observations, which provide reasonably good spatial coverage, but have relatively short time history. A recently available blended dataset [*Randel et al*., 1996] from the National Aeronautics and Space Administration Water Vapor Project (NVAP) provides perhaps the most reliable data on atmospheric moisture. However, this dataset covers the period from 1988 onward and, therefore, cannot be used in analysis of climate variability on decadal to interdecadal time scales. To help clarify the definition, in this study we

consider variations on time scales from 20 years and longer as interdecadal variations, whereas variations on the shorter time scales (but longer than interannual) are considered as decadal variations.

Precipitable water data, (hereafter referred to as PW) starting from 1948 and covering a period of more than 50 years, from the National Centers for Environmental Prediction - National Center for Atmospheric Research (NCEP/NCAR) reanalysis [*Kalnay et al.*, 1996], have become available and provide an opportunity to investigate long-term atmospheric moisture variations. Because the background state of sea surface temperature (SST) has undergone a rapid transition from a cold epoch to a warm epoch in the mid-1970s [*Nitta and Yamada*, 1989; *Tanimoto et al*., 1993; *Graham*, 1994; *Trenberth and Hurrel*, 1994], it remains interesting to see whether this interdecadal variation is also reflected in the atmospheric moisture.

Using data for the 17-year period 1979-1995, *Trenberth and Guillemot* [1998] found some biases in climatology and interannual variability of PW in the reanalysis dataset. In particular, it was shown that over the western tropical Pacific and Indonesian maritime continent, the atmosphere in the reanalysis dataset is drier than that in the NVAP dataset. Assuming that the dry bias in the reanalysis dataset is consistent throughout the time, this effect would be minimized because the focus of this study is not to evaluate the absolute accuracy of the reanalysis dataset but rather to investigate how the long-term climate variations are presented in PW in the reanalysis dataset and what is their spatio-temporal structure.

In the present study we analyze long-term climate variations in the global tropics on the basis of relatively continuous-in-time and spatially homogeneous data on PW

available from the NCEP/NCAR reanalysis. The data used and analysis methods are described in section 2. Intercomparison of dominant modes of PW variability with those of precipitation from satellite estimation for 1979-1998, is presented in section 3. Climatology and general features of total year-to-year variability of annual mean PW are discussed briefly in section 4. Dominant modes of PW variability defined by empirical orthogonal functions (EOF) analysis are analyzed in section 5. Section 6 examines variability of regionally averaged PW. Finally, concluding remarks are presented in section 7.

2. Data

The main data source for this study is the NCEP/NCAR reanalysis [*Kalnay et al*., 1996; Kistler et al., 2001], which is the result of the outstanding project to produce dynamically consistent synoptic scale resolution fields of the basic atmospheric quantities and computed parameters for the needs of climate studies. NCEP/NCAR reanalysis provides parameters for 6-hourly temporal resolution and 2.5º latitude by 2.5º longitude spatial resolution for a 51-year period (1948-1998). The reanalysis project uses a frozen assimilation technique to analyze past data and gives the possibility to explicitly describe short and long-term climate variability within the uncertainties introduced by the changes in the input data. Pressure-level data as well as surface data at 2.5° grid are considered to be instantaneous values at the reference time.

Monthly averaged precipitation data from the Climate Prediction Center Merged Analysis of Precipitation (CMAP) data set [*Xie and Arkin*, 1996, 1997] cover a time period from January 1979 to December 1999. The data have 2.5? latitude by 2.5?

longitude spatial resolution. Values are obtained from 5 kinds of satellite estimates (GPI, OPI, SSM/I scattering, SSM/I emission and MSU). These data are believed to be the most reliable data on precipitation and, therefore, can be useful in validation of the quality of reanalyses products.

In our analysis we used the monthly precipitable water content (i.e., the total column water vapor) from NCEP/NCAR reanalysis for 1948-1998. Though these data, as was mentioned, may have some biases, in comparison to other hydrologic variables they have potential advantages too. First, in contrast to observations from a small number of raingages, which are located at irregular locations with varying record length in the tropics, the PW has the advantage of being spatially homogeneous and of common length of observations at each grid point. Widely used alternative sources of satellite (remote sensing) estimation, which have high resolution in time and space such as the NVAP dataset mentioned previously, cover only periods of 12 years or so at the best. Second, other rainfall-related data from NCEP/NCAR reanalysis, such as model-derived outgoing longwave radiation (OLR) or precipitation rate, are classified as C data. That means that there are no observations directly affecting these variables and therefore, these data are purely model simulated. PW in NCEP/NCAR reanalysis is classified as B data, indicating that there were observational data that directly affected the value of the variable [*Kalnay et al*. 1996]. Third, in terms of seasonal means, PW demonstrates essentially higher agreement with precipitation from the CMAP data set [*Xie and Arkin*, 1996, 1997] than model derived rainfall and OLR [*Randel et al*., 1996; *Martin*, 1999; *Newman et al*., 2000]. Note that the CMAP dataset covers only about 20 years of record length, a period too short to study decadal to interdecadal variations.

When and where it was possible, we compared our results with variability of other hydrologic variables and with results of other studies. In particular, we used CMAP data [*Xie and Arkin*, 1996, 1997]. The domain of analysis in this study is the global tropics between 30°N and 30°S. To check the consistency of PW between the reanalysis and actual observation, specific humidity at 850 hPa and surface-to-500 hPa precipitable water at two stations are also used. The data were downloaded from NOAA Air Resources Laboratory website, and are described in Ross and Elliott [2001]. These data are based on the NCAR upper-air archive and are a subset of the Comprehensive Aerological Research Data Set [CARDS; Eskridge et al. 1995; Wallis, 1998]. Note that the aforementioned website covers data only for the Northern Hemisphere. Furthermore, precipitable water are available for 1973-1995 and specific humidity for 1958-1995.

3. Intercomparison of dominant modes of PW and CMAP variability

In order to investigate how well interannual variability is presented in PW in the global tropics, we performed EOF analysis on time series of the monthly means (with annual cycle removed) of reanalysis PW and precipitation from CMAP for the period January 1979 – December 1998. Spatial patterns of the first two EOF modes are presented in Fig. 1. Time series of the corresponding time-dependent coefficients are shown in Fig. 2.

The first EOF mode accounts for 12.9% of the total variance of PW and 11.5% of the total variance of precipitation. Respective spatial patterns (Figs. 1a,b) show major action centers over the central/eastern tropical Pacific and western tropical Pacific/Indonesian maritime continent. We note that the action center of PW over the

central/eastern tropical Pacific is shifted to the east relative to the precipitation pattern. Although PW and precipitation are closely related variables of the climate system, it should be noted that PW is not precipitation and some differences between PW and precipitation fields are expected. Therefore, some discrepancy between PW and precipitation is expected. Returning to Figs. 1a and b, the secondary action center over the northeastern Brazil seen in precipitation is not well captured by the first EOF mode of PW. The spatial correlation between the two patterns (Figs. 1a and b) is 0.71, which is statistically significant at the 99% confidence level according to t-test [*Bendat and Piersol*, 1966]. Time series of the corresponding time-dependent coefficients (Figs. 2a,b) demonstrate very similar temporal behavior. They are also highly and significantly correlated (0.88). The time series exhibit interannual variations (Figs. 2a,b) associated with the El Niño-Southern Oscillation (ENSO), which is the major climatic signal in the tropics. Particularly, remarkably high positive time-dependent coefficients occur in 1983 and 1998 (Figs. 2a,b), indicating the influence of strong El Niños on PW and precipitation.

The second EOF mode explains 6.9 % of the total variance of PW and 6.0% of the total variance of precipitation. Respective spatial patterns (Figs. 1c,d) are characterized by the very similar wave number two structures with coherent changes over the eastern tropical Pacific, the Indonesian maritime continent and major portion of the Indian Ocean. The opposite changes are evident in the third action center over the central tropical Pacific north of the equator (Figs. 1c,d). Spatial correlation between these two patterns is 0.51 and is statistically significant at the 99% confidence level. Time series of the respective corresponding time-dependent coefficients (Figs. 2c,d) are also well

correlated (0.68). Both series exhibit large excursions during the major ENSO events (i.e., 1982/1983 and 1997/1998). Just like the first EOFs, the second EOFs of PW and CMAP have some ENSO-like features which are expected for an EOF analysis of a field with significant temporal variations. The similarities of dominant modes between the PW and CMAP for the 1979 to 1998 period imply that PW analysis which follows for the extended 1948 to 1998 period may also be representative of the concurrent large-scale precipitation variations.

4. Climatology and temporal variability of PW since 1948

The climatological annual mean PW distribution based on the period of 1948-1998 is shown in Fig. 3a. Maximum values of the PW reaching 45 kg/m² are located over the western tropical Pacific, the Indonesian maritime continent, and the eastern Indian Ocean. Smaller pockets of the maximum PW are also observed in the equatorial eastern Pacific and over equatorial Africa and South America. In general, the belt of high values of PW is associated with location of the intertropical convergence zone (ITCZ) characterized by enhanced convective activity. The pattern revealed in Fig. 3a qualitatively agrees well with the radiosonde-based climatology of *Peixoto and Oort* [1992], 5-year (1988-1992) climatology published by *Randel et al.* [1996], and climatology of precipitation from CMAP [*Xie and Arkin,* 1996, 1997]. Spatial correlation between the CMAP rainfall and reanalysis PW is high (0.73) and is statistically significant at the 99% confidence level.

Total year-to-year variability of PW is shown in Fig. 3b. The values are expressed as a standard deviation (hereafter STD) of annual mean PW. Relatively high variability

of PW is evident in the central and eastern equatorial Pacific and is associated with changes in the tropical circulation patterns related to the ENSO phenomenon. Two other regions of relatively high PW variability are the Indonesian maritime continent and central Brazil. Regarding the large variability over North Africa between 10ºN and 20ºN, it is unclear whether this variability represents a true climate signal because this region is poorly covered with actual observations. This point will be discussed later.

5. Leading modes of variability of PW since 1948

To further investigate the dominant modes of year-to-year variability of PW in the global tropics, we applied EOF analysis to the entire time series of the annual mean PW (1948-1998). Only the first two EOFs are separated reasonably well with respect to sampling errors (North et al., 1982) and are relatively stable. These two EOFs jointly explain 37.3 % of the total variance of PW. Spatial patterns of the first two EOF modes are presented in Fig. 4. Time series of the amplitudes of the leading two eigenvectors and their respective 5-year running means are shown in Figs. 5a,c. Power spectra estimated for these time series and the 95% confidence limit of the red noise spectrum are presented in Figs. 5b,d. The Parzen lag window is used to smooth the sample spectrum [*Chu and Katz*, 1989].

The first EOF mode accounts for 25.4% of the total variance of annual mean PW. The spatial pattern shows four major action centers: over the South America/tropical eastern Pacific, the equatorial central Pacific, the Indonesian maritime continent, and North Africa (Fig. 4a). While the variation of PW over the Indonesian maritime continent and the South America is in phase, it is opposite to that over Africa, most of the Indian

Ocean and a large portion of the tropical central-western Pacific Ocean. The corresponding time-dependent coefficients (Fig. 5a) show an evident downward trend from positive anomalies during the 1950s and 1960s to negative anomalies in the mid 1970s and later. Thus, an interdecadal variation is seen. In analyzing the annual mean precipitable water using radiosonde records over the Northern Hemisphere (mostly midlatitudes), *Ross and Wang* [2000] also noted that the leading EOF mode represents the long-term trend. The spectrum of the first EOF time series (Fig. 5b) shows that a large portion of power is indeed found in the lower frequency, a feature also implied by the trend as seen in Fig. 5a. In Fig. 5b, except for the long-term trend, only a minor peak with periods of 3-3.5 years is marginally significant relative to the red noise spectrum. Although there is agreement between the long-term trend indicated in Fig. 5a and results of some previous observational studies [*e.g. Gaffen et al.,* 1991], it should be cautioned that the observed trend may be associated with the changes in the observing system [*Kistler et al.,* 2001]. We will discuss this point in more detail in the discussion and concluding remarks.

The second EOF has a different structure from the first mode and explains 11.9 % of the total variance of annual mean PW. Its spatial pattern is characterized by the prominent Pacific dipole (Fig. 4b), with the strongest signal being in the central/eastern tropical Pacific, and opposite variations evident in the western tropical Pacific. Relatively small minor action centers are located over the south Atlantic and the northern Africa. Time series of this eigenmode exhibit interannual variations (Fig. 5c) associated with the ENSO. In particular, remarkably high positive values during 1983 and 1998 (strong El Niño years) indicate that the troposphere over the western tropical Pacific was

drier than usual, while Southeast Asia, the bulk of the tropical Pacific, and South America were anomalously moist (Fig. 4b). Correlations between the second EOF time series and SST series in Niño 3 and Niño 3.4 regions are high (0.72 and 0.69 respectively) and are statistically significant at the 95% confidence level. Spatio-temporal structure of this mode is consistent with the second EOF mode obtained by *Gaffen et al*. [1991] from analysis of specific humidity in the global tropics.

The power spectrum of time-dependent coefficients of the second EOF mode (Fig. 5d) shows that only variations with a time period near 4 years (ENSO time scale) are statistically significant. However, decadal scale variations are also evident (especially in the smoothed time series in Fig. 5c), indicating a change of phase from negative to positive PW anomalies over the major portion of the global tropics in the mid-1970s. Timing of this change suggests its association with the well known North Pacific climate shift that occurred in the mid 1970s, as diagnosed from analyses of SST and atmospheric variables [*Nitta and Yamada,* 1989; *Tanimoto et al*., 1993; *Graham*, 1994; *Trenberth and Hurrel*, 1994]. This temporal shift in EOF-2 time series is also approximately coincidental with the addition of a significant amount of satellite data to the analysis (Kistler et al., 2001).

To determine whether the decadal change in PW EOF-2 time series is significant, a common two-sample t-test is applied to the periods of 1948-1976 and 1977-1998 (Wilks, 1995). Under the assumption of independence, the test statistic z is –2.42, which corresponds to an extremely small p value, 0.0078. Thus, the null hypothesis that the two underlying means are equal is rightfully rejected. Because geophysical time series usually exhibit strong persistence, the number of sample sizes that correspond to the

temporal degrees of freedom should be adjusted. One way to determine the "effective sample size" is to assume that the underlying data follow a first-order autoregressive process (e.g., Shukla and Mo, 1983). After temporal degrees of freedom are properly adjusted, the p value of the test statistic becomes 0.0162, and the null hypothesis of equality of sample means is again rejected at the 5% level. Results of these two tests strongly support a significant difference in the means of PW EOF-2 series pre- and post-the mid-1970s (Fig. 5c).

As very large variability over North Africa is present in both EOF modes (Figs. 4a,b), a question arises as to whether this variability might bias results of EOF analysis. To examine the possible effect of this region on the analysis, we excluded Africa and performed EOF analysis for the same global tropical band extending from 40ºE eastward to 0ºE for the period of 1948-1998. Explained variance for the newly estimated first EOF mode appeared lower (20.8%), whereas for the second EOF the explained variance is higher (13.5%) than in the EOF analysis for the whole global tropics. However, obtained spatial patterns and their time-dependent coefficients for the first and second EOF modes (not shown) appeared qualitatively similar to those presented in Figs. 4 and 5. Specifically, the spatial correlation of the first EOF mode between the global tropical band and the same region but without North Africa is 0.97. The temporal correlation of the first EOF time series between these two datasets is also very high, 0.911. Likewise, for the second mode, the spatial and temporal correlations are 0.879 and 0.937, respectively. All correlations are significant at 99% confidence level. Thus, large local variability of the annual mean PW over North Africa did not have a noticeable effect on the overall results of the EOF analysis presented in Figs. 4 a and b.

The aforementioned behavior of time-dependent EOF coefficients reflects overall tendencies of PW for the global tropics; however, regional differences are remarkable. In order to examine these differences, in the next section we consider temporal behavior of regionally averaged annual mean PW.

6. Regional changes in the action centers since 1948

To analyze regional changes in PW, we constructed time series of regionally averaged anomalies of the annual mean PW for the period of 1948-1998. Based on results of EOF analyses shown previously, four regions associated with major action centers of the first EOF mode (Fig. 4a) were selected. These regions include North Africa (10ºN-20ºN, 10ºE-20ºE), Malaysia (0º-10ºN, 100ºE-110ºE), the central equatorial Pacific (0º-10ºN, 155ºW-165ºW), and central Brazil (5ºS-15ºS, 45ºW-55ºW). In each region, data from 25 grid points were used to estimate regional averages. Time series of anomalies of annual mean PW and their 5-year running means for each of these regions are shown in Figs. 6a,c,e,g. Respective power spectra for these time series and the 95% confidence limit of the red-noise spectrum are presented in Figs. 6b,d,f,h.

As seen in all four regions, time series of PW anomalies demonstrate well pronounced interdecadal changes (Figs. 6a,c,e,g), which were described, in general, by the first two EOF modes (Figs. 4 and 5). However, temporal behavior of presented time series and the character of interdecadal changes are different at various locations.

Temporal behavior of PW over North Africa is featured by positive anomalies in the first twenty years, followed by an abrupt decrease of PW in the late 1960s (Fig. 6a) with persistent, negative anomalies remaining until 1998. The magnitude of this change

is the largest among all four time series analyzed (Figs. 6a,c,e,g). In general, this decadal change is consistent with the long-term rainfall behavior in Sahel in which positive rainfall anomalies in the 1950s changed to negative anomalies in the 1960s and the below normal rainfall subsequently remained to the early 1990s [*Nicholson et al*., 1996]. Also note in Fig. 6a, year-to-year variability of annual mean PW is very high during the 1950s and 1960s and relatively low since the late 1960s. Because North Africa is characterized by an arid climate, large PW fluctuations in the earlier part of the record (Fig. 6a) may not be realistic. In fact, this extreme maximum variability of annual mean PW is not seen in the NCEP/NCAR reanalysis for the period 1979-1998 (Fig. 2a). Considering all these facts, it is most likely that abrupt excursions in PW over North Africa are associated with changes in the observing system. The respective power spectrum (Fig. 6b) shows that in this region energy is concentrated at the very low frequency end, reflecting a trend behavior. Only variations with time period near 3 years are marginally significant at 95% confidence level.

Anomalies of the annual mean PW over Malaysia changed from negative to positive ones in the late 1970s (Fig. 6c). The time series demonstrates step-like change in PW that coincides with the introduction of satellite data. The respective power spectrum (Fig. 6d) does not reveal any statistically significant peaks.

Variability of annual mean PW over the equatorial central Pacific is characterized by intensive interannual variations associated with ENSO and by long-term trend-like decrease of PW over the region (Fig. 6e). This result corroborates our earlier analysis presented in Figs. 4a and 5a. The power spectrum in Fig. 6f demonstrates that in this

region only ENSO-related PW variations with a period near 4 years are statistically significant at 95% confidence level.

Long-term behavior of PW anomalies over central Brazil is marked by a nearly low-frequency variation (Fig 6g). Low PW conditions in this region prevailed from the mid-1950s to the mid-1970s and then were replaced by anomalously moist conditions thereafter. The estimated power spectrum (Fig. 6h) shows that variations with periods of 5-9 years are statistically significant in this region. Adjacent to central Brazil is the Amazon basin where maximum annual mean PW is noted (Fig. 3a). In the Amazon basin, temporal behavior of the PW is similar to central Brazil, with more moisture since the mid-1970s (not shown). We note that *Chu et al*. [1994], using 15-year (1974-1990 with a gap in 1978) records, found significant OLR decrease with time (i.e., an increase in tropical convection) over the extreme western Amazon basin. They also reported a concurrent upward trend in precipitation at Belem (1.5ºS, 48.5ºW) and Manaus (3.2ºS, 60.0ºW). However, interdecadal changes presented in Fig. 6g could be biased by the aforementioned changes in the observing system.

In order to compare the aforementioned time series of PW with purely observational data, we present in Fig. 7 time series of annual means of specific humidity at 850 hPa and surface-to-500 hPa precipitable water at two WMO (World Meteorological Organization) stations that are close to our key regions. The stations selected include Lihue, Kauai in Hawaii (21.98°N, 159.35°W) and Haikou in China (20.02°N, 110.21°E). The former station is closest to our key region in the central equatorial Pacific and the latter is closest to another key region over Malaysia. Singapore, which is closer to Malaysia than Haikou, does have upper-air records but they

are inaccessible to us. For the other two key regions - central Brazil and North Africa – we were not able to construct time series of observed specific humidity or precipitable water. This is because radiosonde stations in these regions are located either in the Southern Hemisphere for where data are not available from the NOAA Air Resources Laboratory website or have incomplete and inhomogeneous temporal records. Ross and Elliott [2001] showed that specific humidity at 850 hPa level and surface-to-500 hPa precipitable water are highly correlated with little geographic variations in their relationships. Therefore, specific humidity at lower troposphere can serve as a useful surrogate for precipitable water.

The upward trends in atmospheric moisture are most pronounced since the mid-1970s at both stations (Fig. 7). Trends at Haikou station are consistent with the upward PW fluctuations over Malaysia (Fig. 6c). However, trends at Lihue, Kauai, tend to be opposite to PW trend over central equatorial Pacific (Fig. 6e). Apart from the latitudinal distance between Lihue and the central equatorial Pacific, the downward trend revealed in Fig. 6e may be attributable to a quality problem in reanalysis over the data-sparse region such as the central equatorial Pacific where no radiosonde stations can be found.

To trace changes in the number of radiosonde observations over North Africa, we examined a digitized metadata set of global upper-air station histories developed by Gaffen [1996]. During the 1960s and early 1970s many countries in this region became independent. As a result, many stations were closed and re-opened several times. Therefore, it is extremely difficult to judge whether the total number of observations over North Africa decreased or increased. A further complication to the problem is changes in observational instrumentations. In sum, upper-air observations over North Africa are

incomplete and inhomogeneous in both space and time and thus are not suitable for analysis of long-term climate variations. Such changes in observing practices could affect the reanalysis product in this region.

7. Discussion and concluding remarks

We analyzed climatic variability of the annual mean PW (tropospheric precipitable water) in the global tropics based on data from the NCEP/NCAR reanalysis [*Kalnay et al*., 1996]. Climatology of annual mean PW agrees well with earlier published climatologies based on data from other sources [*Peixoto and Oort*, 1992; *Randel et al*., 1996]. In particular, major maxima of the annual mean PW are observed over the western tropical Pacific/Indonesian maritime continent, the equatorial eastern Indian Ocean, the Amazon Basin, and over equatorial Africa. Year-to-year variability in PW is relatively large over North Africa, the Indonesian maritime continent, the equatorial central Pacific, and central Brazil.

The first EOF mode of the entire time series (1948-1998) reflects interdecadal changes in the annual mean PW in the global tropics, as implied by a downward trend with positive anomalies during the 1950s and 1960s and negative anomalies since the 1970s. There is a certain similarity between this mode and the second EOF mode of precipitation obtained by *Lau and Sheu* [1991] from analysis of global station rainfall data from 1901-1980. *Krishnamurthy and Goswami* [2000] demonstrated that during the warm phase of interdecadal SST variations the equatorial Pacific and Indian oceans are marked by two large Walker cells, with anomalous ascending motion in the eastern Pacific and central Indian (near 90ºE) oceans joined by an intensified descending motion

in the central Pacific (their Fig. 18a). The latter results in anomalously dry conditions in the region. The decrease in PW over the equatorial central Pacific as seen in Fig. 6e, and as also inferred from the spatial pattern and the time-dependent coefficients of the first EOF mode (Figs. 4a and 5a), is consistent with the mechanism of interdecadal changes in the tropics proposed by *Krishnamurthy and Goswami* [2000]. Nevertheless, there are indications that the obtained trend in tropical PW resulted from pronounced changes in the evolving observing system.

Kistler et al. [2001] separate the evolution of the global observing system into three major phases: the "early" period from 1940s to International Geophysical Year in 1957, when the first global-scale upper-air observations were established; the "modern rawinsonde network" from 1958 to 1978; and the "modern satellite" era from 1979 to the present. Note that most of the time series considered in the present study demonstrate step-like changes in PW in the mid-late 1970s. These changes basically coincide with the introduction of satellite data. Moreover, our intercomparison analysis of dominant modes of PW and CMAP variability (Section 3) during 1979-1998 does not reveal any noticeable long-term trends for that period (Fig. 2). Therefore, consistent with *Kistler et al.* [2001], our results suggest that the primary reason for the detected interdecadal trend associated with the first EOF mode is the changes in the observing system during the past decades.

Based on the entire time series, the second EOF mode of the annual mean PW in the global tropics is associated with ENSO. Its spatial pattern is characterized by the dipole-like structure over the tropical Pacific Ocean. The spatial pattern and temporal behavior of the corresponding time-dependent coefficients are very similar to those of the

second EOF mode of the tropical specific humidity obtained by *Gaffen et al*. [1991] from analysis of radiosonde data. In general, both analyses show that the air over the western Pacific was drier than usual during El Niño years, whereas the central-eastern Pacific, South America, and Southeast Asia were anomalously moist.

The smoothed time series of the second EOF mode also demonstrate a change from negative to positive PW anomalies over most of the global tropics in the mid-1970s. The average PW EOF-2 time series for the period prior to mid-1970s is significantly different from that after mid-1970s even when the reduction of effective degrees of freedom due to persistence is taken into account. Timing of this change suggests that it is associated with the previously described Pacific climate shift, which is considered as a manifestation of the Pacific decadal oscillation [*Mantua et al.*, 1997]. During this warm decadal phase, SST decreased in the extratropical North Pacific and increased in the tropical Pacific and Indian oceans. This change of SST in the tropical Pacific and Indian oceans is also interpreted as a manifestation of decadal components of ENSO [*Zhang et al.*, 1997]. Therefore, at the decadal time scale, our analysis demonstrates a general level of increase of PW over almost the entire global tropics in response to the increase of SST since 1976/77, although further analyses are needed to quantify the PW-SST relationships.

Analysis of regional time series of the annual mean PW anomalies since 1948 indicates that interdecadal changes are present in all four centers of action. However, regional differences in temporal behavior of PW are evident. Interdecadal changes of the annual mean PW over Malaysia and the central tropical Pacific are presented, respectively, by conspicuous upward and downward trends. Meanwhile, changes over

central Brazil at the given time scale show a low-frequency variability with lower than time-mean PW from the late 1950s to the late 1970s and higher than time-mean PW during the later time period. However, PW variations in all three above regions demonstrate step-like changes in the late 1970s, suggesting that described trends are associated with the introduction of satellite data.

Interdecadal changes in the annual mean PW over North Africa feature an abrupt decrease of PW in this region in the late 1960s. The magnitude of this change is the largest among the four action centers. While the decrease of PW is parallel to long-term rainfall variations in Sahel, it seems that such a high magnitude of change is not realistic for a region characterized by arid climate. It is speculated that changes of PW over North Africa are unreliable during the earlier period of records (1950s-1970s) because of the irregularity in observing practices.

The results of intercomparison of PW and CMAP precipitation variability during the past 20 years (1979-1998), when PW values are more reliable, indicate that year-to-year variability of PW in the global tropics is reasonable in the reanalysis. However, because of the major change in input data in the late 1970s (i.e., satellites versus no satellites) which occurred nearly concurrently with the real climate shift in the Pacific, it is difficult to study interdecadal PW variations using reanalysis data sets.

Summarizing results of the present study we note that this is the first time the reanalysis PW climatology and PW variability over the last fifty years (1948-1998) have been studied. As previously mentioned, this data set has utility for climate studies because of its relative homogeneity, long and common length of records, and the global coverage. Intercomparisons with satellite-derived and some radiosonde-based data are

made in order to assess the quality of reanalysis PW in the global tropics. New results from this study indicate that although there is a potential dry bias in the reanalysis PW, as pointed out by others, the PW data can be used for analysis of climate variability since the mid-1970s as long as the absolute accuracy of this variable is not of essence. The usage of the earlier (pre-satellite era) data is, nevertheless, problematic.

Acknowledgments

We are grateful to Dr. Julian Wang for his helpful comments and suggestions on the first draft of this manuscript and Di Henderson for her technical editing. Our sincere thanks also go to two anonymous reviewers, who helped improve the presentation of this paper greatly. Funding from the Frontier Research System for Global Change to IIZ is greatly appreciated. Partial funding for PSC comes from NOAA Cooperative Agreement Number NA17RJ1230. IIZ was also supported by the Russian Foundation for Basic Research (Grant 02-05-64498). This paper is SOEST contribution 6068.

References

Angell, J.K., W.P. Elliott, and M.E. Smith, Tropospheric humidity variations at Brownsville, Texas, and Great Falls, Montana, 1958-80, *J. Climate Appl. Meteor.*, 23, 1286-1296, 1984.

Bendat, J.S., and A.G. Piersol, *Measurement and Analysis of Random Data*, 390 pp., J. Wiley & Sons, 1966.

Chu, P.-S., and R.W. Katz, Spectral estimation from time series models with relevance to the Southern Oscillation, *J. Climate*, 2, 86-90, 1989.

Chu, P.-S., Z.-P. Yu and S. Hastenrath, Detecting climate change concurrent with deforestration in the Amazon basin: Which way has it gone?, *Bull. Amer. Meteorol. Soc.*, 75, 579-583, 1994.

Eskridge, R.E., and coauthors, A Comprehensive Aerological Reference Dataset (CARDS): Rough and systematic errors. *Bull. Amer. Meteor. Soc*., 76, 1759-1775, 1995.

Flohn, H., and A. Kapala, Changes of tropical sea-air interaction processes over a 30-year period, *Nature*, 338, 244-246, 1989.

Gaffen, D.J., A digitized metadata set of global upper-air station histories. NOAA Tech. Memo. ERL ARL-211, 38 pp, 1996.

Gaffen, D.J., T.P. Barnett, and W.P. Elliott, Space and time scales of global tropospheric moisture, *J. Climate*, 4, 989-1008, 1991.

Graham, N.E., Decadal-scale climate variability in the tropical and North Pacific during the 1970's and 1980's: Observations and model results, *Climate Dyn*., 10, 135-162, 1994.

Hense, A., P. Krahe, and H. Flohn, Recent fluctuations of tropospheric temperature and water vapor in the tropics, *Meteor. Atmos. Phys.,* 38, 215-227, 1988.

Kalnay, E., Kanamitsu, M., Kistler, R., Collins, W., Deaven, D., Gandin, L., Iredell, M., Saha, S., White, G., Wollen, J., Zhu, Y., Chelliah, M., Ebisuzaki, W., Higgins, W., Janowiak, J., Mo, K. C., Ropelewski, C., Wang, J., Leetma, A., Reynolds, R., Jenne, R. and D. Joseph, The NCEP/NCAR 40-year reanalysis Project. *Bull. Amer. Met. Soc.*, 77, No. 3, 437-471, 1996.

Kistler, R., Collins, W., Saha, S., White, G., Wollen, J., Kalnay, E., Chelliah, M., Ebisuzaki, W., Kanamitsu, M., Kousky, V., van den Dool, H., Jenne, R., Fiorino, M., The NCEP/NCAR 50-year reanalysis: monthly means CD-ROM and documentation. *Bull. Amer. Met. Soc.*, 82, No. 2, 247-268, 2001.

Krishnamurthy, V., and B.N. Goswami, Indian monsoon-ENSO relationship on interdecadal timescale, *J. Climate*, 13, 579-595, 2000.

Lau, K.-M., and P.J. Sheu, Teleconnections in global rainfall anomalies: seasonal to inter-decadal time scales, in *Teleconnections Linking Worldwide Climate Anomalies*, edited by M.H. Glantz, R.W. Katz and N. Nicholls, 227-256, Cambridge University Press, 1991.

Mantua, N.J., S.R. Hare, Y. Zhang, J.M. Wallace, and R. Francis, A Pacific interdecadal climate oscillation with impacts on salmon production, *Bull. Amer. Met. Soc.*, 78, 1069-1079, 1997.

Martin, G.M., The simulation of the Asian summer monsoon, and its sensitivity to horizontal resolution, in the UK Meteorological Office Unified Model, *Q.J.R. Meteorol. Soc.*, 125, 1499-1525, 1999.

Newman, M., P.D. Sardeshmukh, and J.W. Bergman, An assessment of the NCEP, NASA, and ECMWF Reanalyses over the West Pacific Warm Pool, *Bull. Amer. Meteorol. Soc.*, 81, 41-48, 2000.

Nicholson, S.E, M.B. Ba, and J.Y. Kim, Rainfall in the Sahel during 1994, *J. Climate*, 9, 1673-1680, 1996.

Nitta, T., and S. Yamada, Recent warming of tropical sea surface temperature and its relationship to the Northern Hemisphere circulation, *J. Meteor. Soc. Japan*, 67, 375-382, 1989.

North, G.R., T.L. Bell, and R.F. Calahan, Sampling errors in the estimation of empirical orthogonal functions, *Mon. Wea. Rev.*, 110, 699-706, 1982.

Oort, A.H., Global atmospheric circulation statistics, 1958-1973. NOAA Prof. Pap. 14, 180 pp., 1983. [Available from U.S. Govt. Printing Office, Washington, DC 20402.]

Peixoto, J.P., and A.H. Oort, *Physics of Climate*. American Institute of Physics, 520 pp., 1992.

Randel, D.L., T.H. Vonder Haar, M.A. Ringerud, G.L. Stephens, T.J. Greenwald, and C.L. Combs, A new global water vapor dataset, *Bull. Amer. Meteorol. Soc.*, 77, 1233-1246, 1996.

Ross, R.J., and W.P. Elliott, Tropospheric water vapor climatology and trends over North America: 1973-93, *J. Climate*, 9, 3561-3574, 1996.

Ross, R.J., and J. Wang, Multi-year variability of tropospheric water vapor. Preprint volume 11th Symposium on global change studies. 9-14 January, Long Beach, California, AMS, Boston, MA., 186-187, 2000.

Ross, R.J., and W.P. Elliott, Radiosonde-based Northern Hemisphere tropospheric water vapor trend, *J. Climate*, 14, 1602-1612, 2001.

Shukla, J., and K.C. Mo, Seasonal and geographical variation of blocking. *Mon. Wea. Rev*. 111, 388-402, 1983.

Tanimoto, Y., N. Iwasaka, K. Hanawa, and Y. Toba, Characteristic variations of sea surface temperature with multiple time scales in the North Pacific, *J. Climate*, 6, 1153-1160, 1993.

Trenberth, K.E., and J.W. Hurrel, Decadal atmosphere-ocean variations in the Pacific, *Climate Dyn*., 9, 303-319, 1994.

Trenberth, K.E., and C.J. Guillemot, Evaluation of the atmospheric moisture and hydrological cycle in the NCEP/NCAR reanalyses, *Climate Dyn.*, 14, 213-231, 1998.

Wallis, T.W., A subset of core stations from the Comprehensive Aerological Reference Dataset (CARDS), *J. Climate*, 11, 272-282, 1998.

Wilks, D.S., *Statistical Methods in the Atmospheric Sciences*, 467pp., Academic Press, 1995.

Xie, P., and P. Arkin, Analyses of global monthly precipitation using gauge observations, satellite estimates, and numerical model predictions, *J. Climate*, 9, 840-858, 1996.

Xie, P., and P. Arkin, Global precipitation: A 17-year monthly analysis based on gauge observations, satellite estimates, and numerical model outputs, *Bull. Amer. Meteorol. Soc.*, 78, 2539-2558, 1997.

Zhai, P., and R.E. Eskridge, Atmospheric water vapor over China, *J. Climate*, 10, 2643-2652, 1997.

Zhang, Y., J.M. Wallace, and D.S. Battisti, ENSO-like decadal variability over the Pacific sector, *J. Climate,* 10, 1004-1020, 1997.

Figure Captions

Figure 1. Spatial patterns of the first (a,b) and second (c,d) EOF modes of monthly anomalies of PW (a,c) and CMAP precipitation (b,d). Intervals between isolines are arbitrary. The period of analysis is 1979-1998.

Figure 2. Time-dependent coefficients (solid curves) of the first (a,b) and second (c,d) EOF modes of monthly anomalies of PW (a,c) and CMAP precipitation (b,d). Dashed curves are the 11-month running means. The period of analysis is 1979-1998.

Figure 3. Climatology (a) and standard deviations (b) of annual mean PW. On both plots values are presented in kg/m^2. The period of analysis is 1948-1998.

Figure 4. Spatial patterns of the first (a) and second (b) EOF modes of annual mean PW. Intervals between isolines are arbitrary. The period of analysis is 1948-1998.

Figure 5. Time-dependent coefficients (a, c) and respective power spectra (b, d) of the dominant EOF modes (solid curves). Dashed curves are the 5-year running means in (a, c), and the 95% significance level of the red noise spectrum in (b, d). The period of analysis is 1948-1998. ENSO years since 1969 are denoted by an open diamond in (c).

Figure 6. Same as Fig. 5, but for time series of regionally averaged annual mean PW for North Africa (a, b), Malaysia (c, d), the equatorial central Pacific (e, f) and central Brazil (g, h). The period of analysis is 1948-1998.

Figure 7. Time sfieries of annual mean specific humidity (g/kg) at 850 hPa (a, c) and surface-to-500 hPa precipitable water (mm) (b, d) at Lihue, Kauai, Hawaii and Haikou, China. The period of analysis is 1958-1995 for specific humidity and 1973-1995 for precipitable water.

a) PW EOF-1 (12.9%)

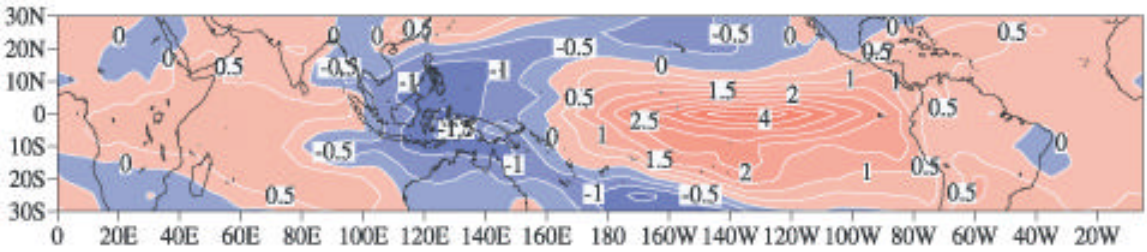

b) CMAP precipitation EOF-1 (11.5%)

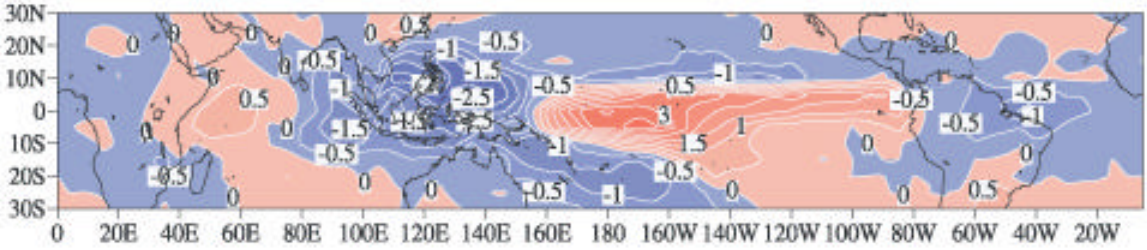

c) PW EOF-2 (6.9%)

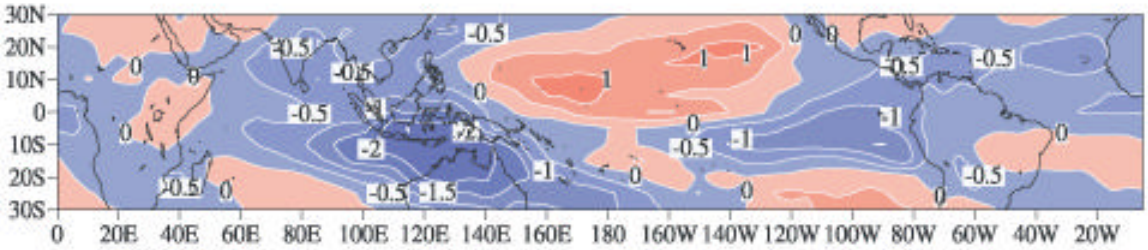

d) CMAP precipitation EOF-2 (6.0%)

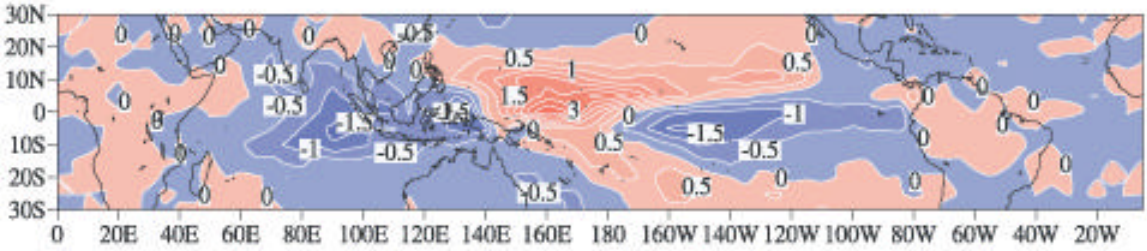

Fig 1.

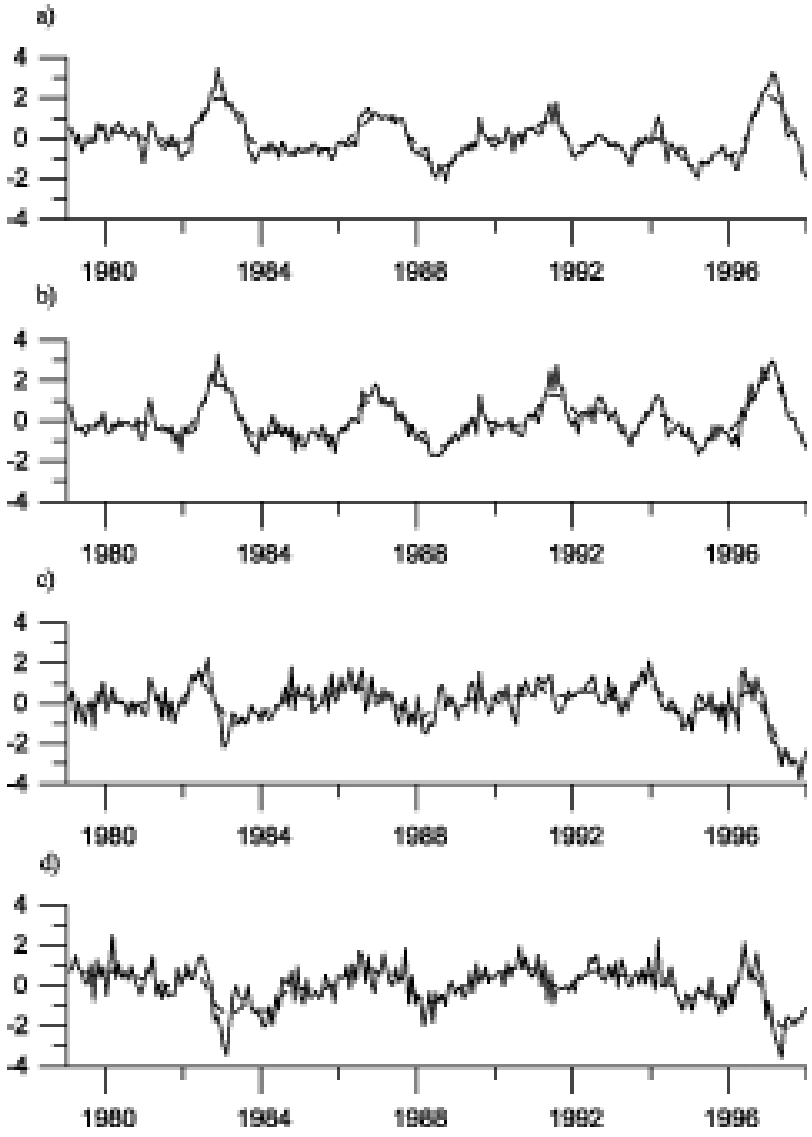
a)
4
2
0
-2
-4
1980
1984
1988
1992
1996
b)
4
2
0
-2
-4
1980
1984
1988
1992
1996
c)
4
2
0
-2
-4
1980
1984
1988
1992
1996
d)
4
2
0
-2
-4
1980
1984
1988
1992
1996

Fig 2.

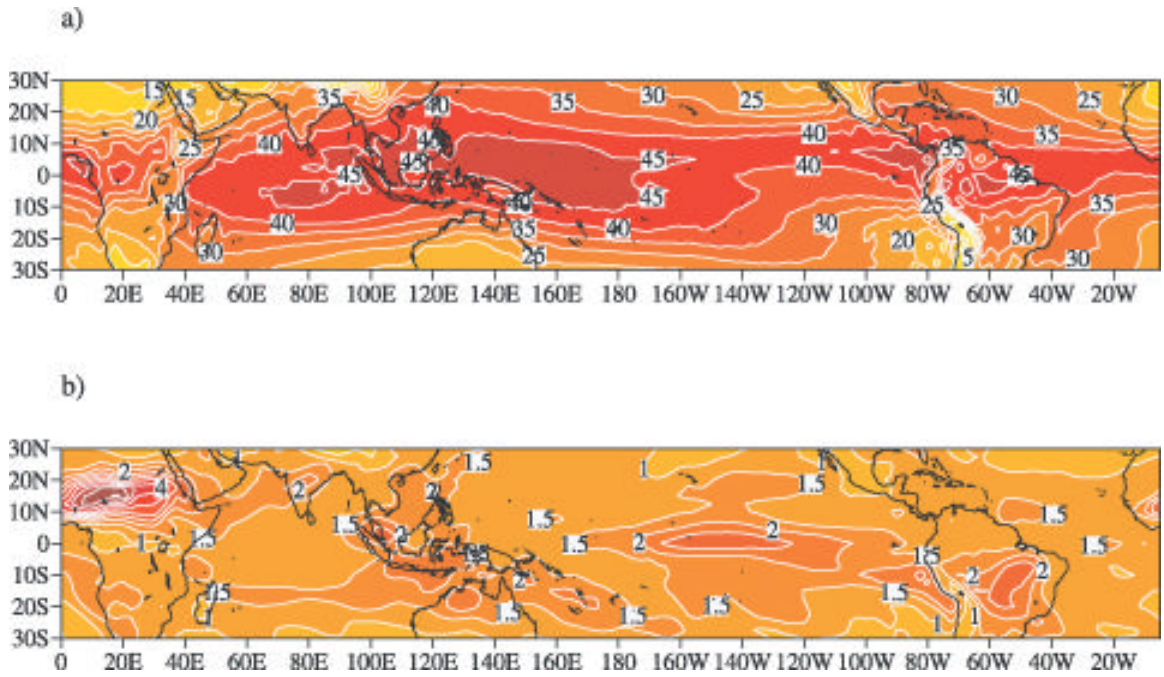
a)
30N
20N
10N
0
10S
20S
30S
0 20E 40E 60E 80E 100E 120E 140E 160E 180 160W 140W 120W 100W 80W 60W 40W 20W
b)
30N
20N
10N
0
10S
20S
30S
0 20E 40E 60E 80E 100E 120E 140E 160E 180 160W 140W 120W 100W 80W 60W 40W 20W

Fig 3

a) EOF-1 (25.4%)

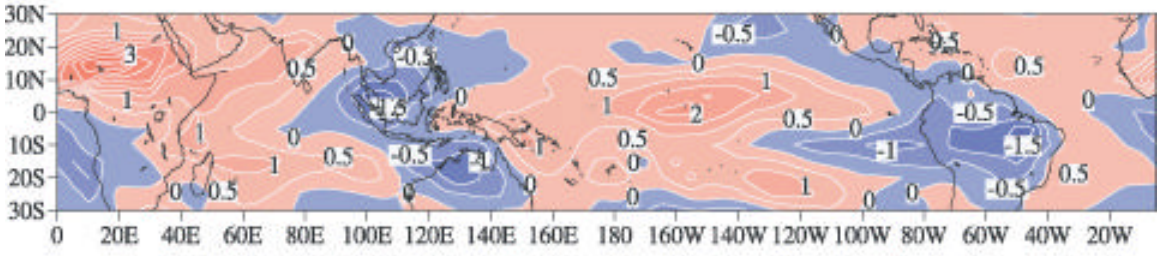

b) EOF-2 (11.9%)

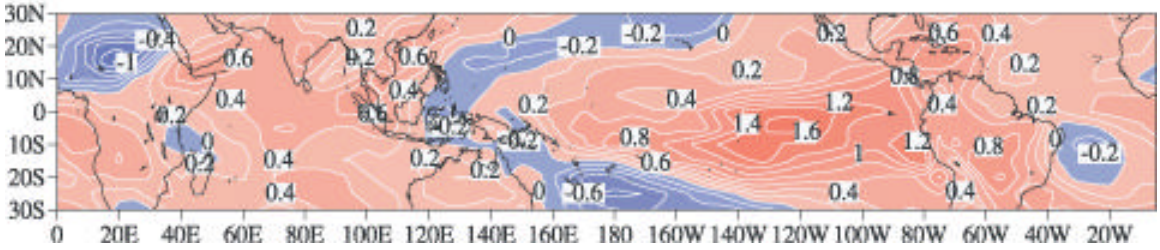

Fig 4

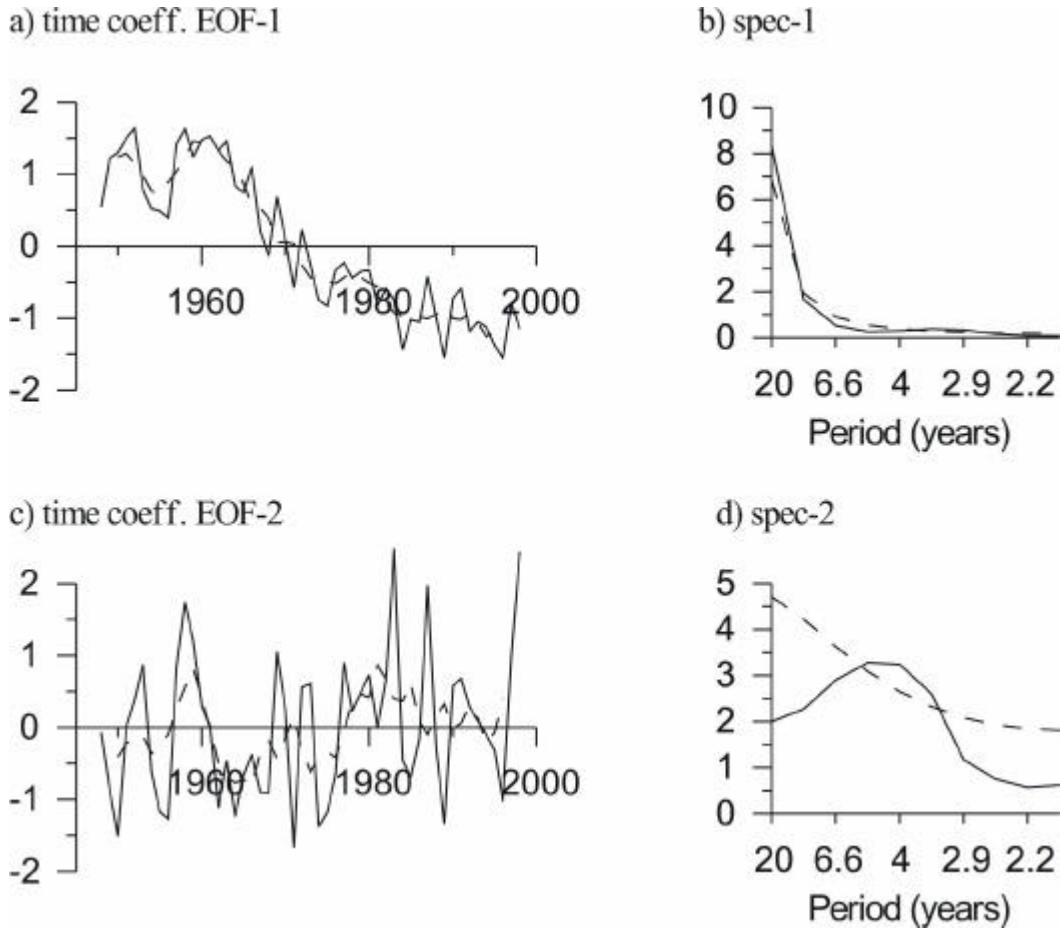
a) time coeff. EOF-1
2
1
0
-1
-2
1960
1980
2000
b) spec-1
10
8
6
4
2
0
20 6.6 4 2.9 2.2
Period (years)
c) time coeff. EOF-2
2
1
0
-1
-2
1960
1980
2000
d) spec-2
5
4
3
2
1
0
20 6.6 4 2.9 2.2
Period (years)

Fig 5

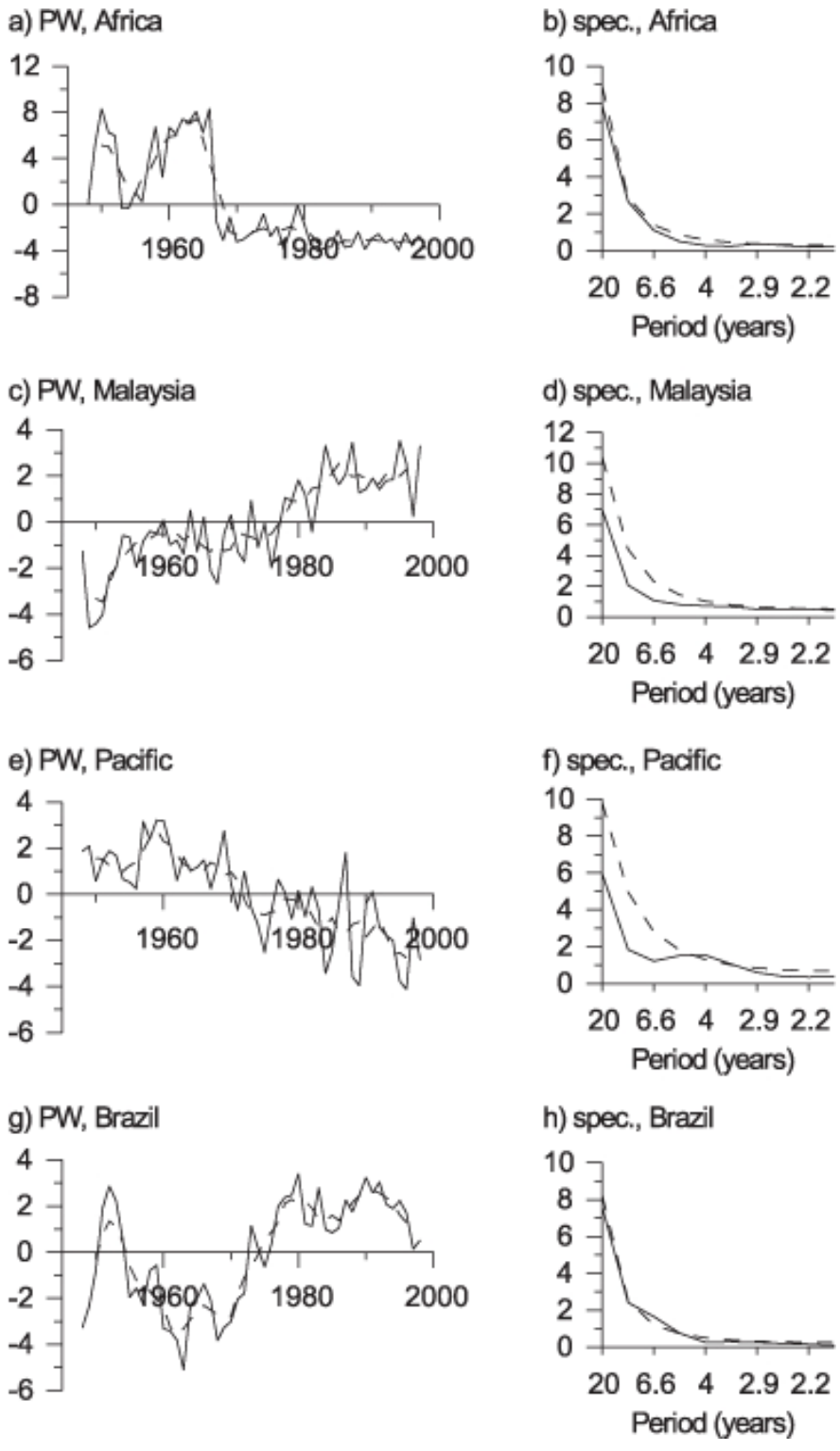
a) PW, Africa
12
8
4
0
-4
-8
1960
1980
2000
b) spec., Africa
10
8
6
4
2
0
20 6.6 4 2.9 2.2
Period (years)
c) PW, Malaysia
4
2
0
-2
-4
-6
1960
1980
2000
d) spec., Malaysia
12
10
8
6
4
2
0
20 6.6 4 2.9 2.2
Period (years)
e) PW, Pacific
4
2
0
-2
-4
-6
1960
1980
2000
f) spec., Pacific
10
8
6
4
2
0
20 6.6 4 2.9 2.2
Period (years)
g) PW, Brazil
4
2
0
-2
-4
-6
1960
1980
2000
h) spec., Brazil
10
8
6
4
2
0
20 6.6 4 2.9 2.2
Period (years)

Fig 6

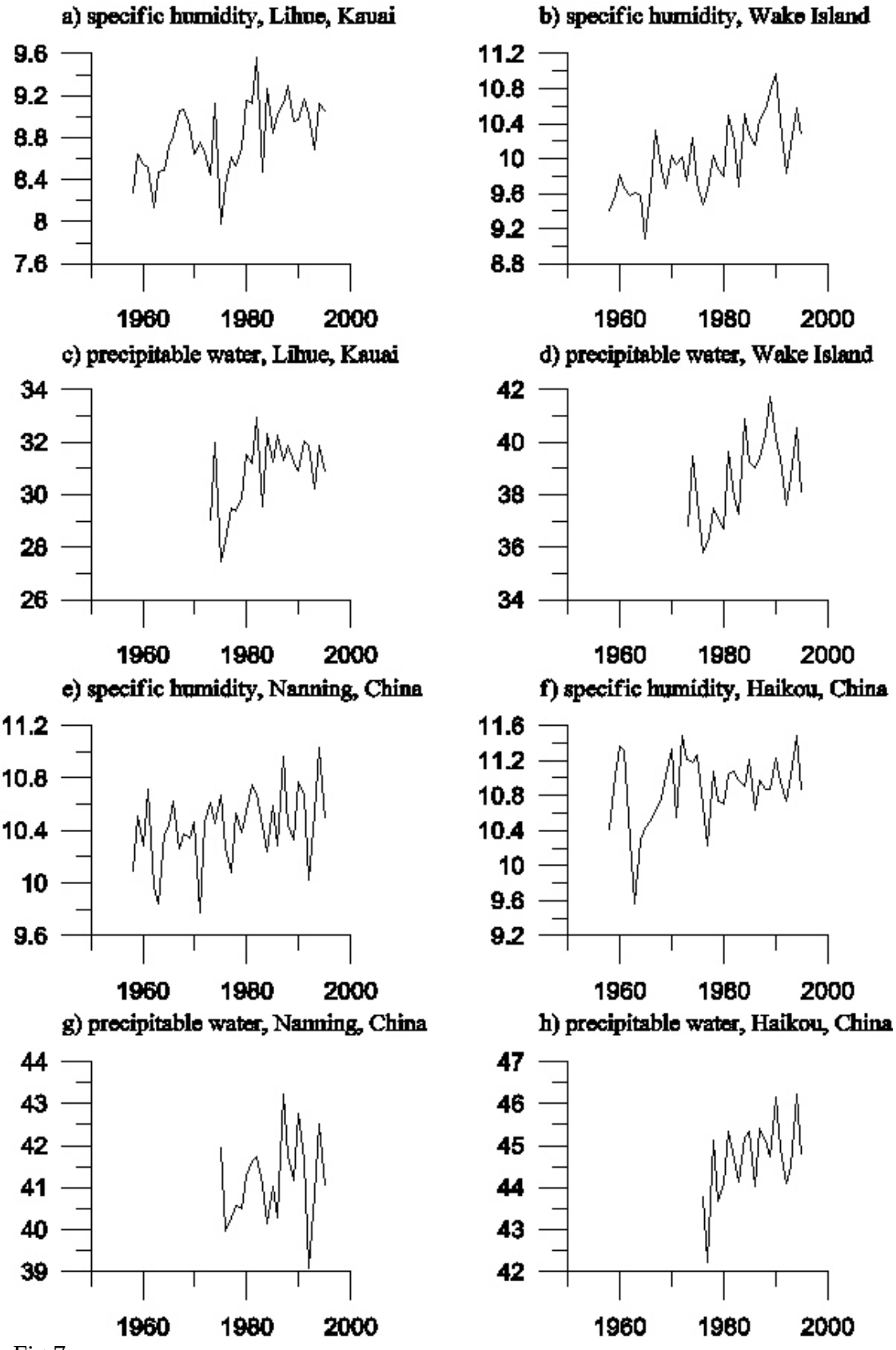
a) specific humidity, Lihue, Kauai
9.6
9.2
8.8
8.4
8
7.6
1960
1980
2000
b) specific humidity, Wake Island
11.2
10.8
10.4
10
9.6
9.2
8.8
1960
1980
2000
c) precipitable water, Lihue, Kauai
34
32
30
28
26
1960
1980
2000
d) precipitable water, Wake Island
42
40
38
36
34
1960
1980
2000
e) specific humidity, Nanning, China
11.2
10.8
10.4
10
9.6
1960
1980
2000
f) specific humidity, Haikou, China
11.6
11.2
10.8
10.4
10
9.6
9.2
1960
1980
2000
g) precipitable water, Nanning, China
44
43
42
41
40
39
1960
1980
2000
h) precipitable water, Haikou, China
47
46
45
44
43
42
1960
1980
2000
Fig 7